

A. ZOLOCHEVSKY, Dr. Sc., National Technical University “Kharkov Polytechnic Institute”, *A. KÜHHORN*, Dr., Brandenburg University of Technology Cottbus, Germany

CONSTITUTIVE AND NUMERICAL MODELING OF CHEMICAL AND MECHANICAL PHENOMENA IN SOLID OXIDE FUEL CELLS AND OXYGEN PERMEABLE MEMBRANES

Виконано моделювання хімічних і механічних явищ, та розроблені узагальнені визначальні співвідношення, які можуть бути використано для розрахунків залежних від часу розподілень напружень та пошкоджуваності, що обумовлена повзучістю, в твердооксидних паливних елементах та в мембранах для переносу кисню як функцій матеріалу та параметрів паливного елемента чи мембрани, які знаходяться в несталих та сталих умовах роботи. Розроблені визначальні співвідношення впроваджено в формі структурних моделей для аналізу розподілу напружень в паливних елементах і в мембранах та деградації в часі, для аналізу міцності та тривалої міцності, для забезпечення безпечної роботи систем паливних елементів та мембран для стаціонарного та транспортного використання.

Constitutive modeling of chemical and mechanical phenomena has been given, and constitutive equations have been developed that will then be used to calculate the time dependent stress distribution and the creep damage growth in Solid Oxide Fuel Cells and in Oxygen Permeable Membranes as a function of material and stack parameters or membrane parameters as well as of operating conditions.

The constitutive model developed has been incorporated in a form of the structural modelling tool for analyzing mechanical stress distributions in the stack or membrane and mechanical degradation over time, for durability analysis and lifetime predictions, and for improving the performance and safety of fuel cells and membranes for transport and stationary applications

Introduction. Molten carbonate and solid oxide Fuel Cells developed at the end of the 20th century push the efficiency of using hydrogen or fuel gas containing hydrogen to generate electric power in the range of 35 to 55 percent of higher heating value. Hydrogen is an ideal fuel and versatile energy carrier, and its advantages are listed as below:

- 1) Renewable, easy to produce,
- 2) Convenient fuel for transportation,
- 3) High utilization efficiency,
- 4) Environmentally compatible (zero- or very low-emission),
- 5) Versatile, converts easily to other energy forms.

Solid Oxide Fuel Cells (SOFCs) consist of an oxygen-ion conducting electrolyte material that is sandwiched in between two thin, porous electrodes [1, 2]. Different cell designs of SOFCs have been studied, including planar, monolithic, segment-cell-in-series and tubular geometries. The cell component materials of the different designs are the same or similar in nature [3-8].

Another application in high-temperature electrochemical devices is Oxygen Permeable Membranes (OPMs) [8-11]. They can be used for direct conversion of methane to syngas at efficiencies > 99%. The major advantage of mixed conductors for this purpose compared to traditional oxygen conducting materials like yttria-

stabilized zirconia is the elimination of the need for an external electric circuit. The operating principle for oxygen permeable membranes is shown in Fig. 1. When the membrane is placed in an oxygen gradient, oxygen is spontaneously transported through the membrane from the high- pO_2 to the low- pO_2 side. Oxygen can then be produced directly from high-pressure air given that the oxygen partial pressure on the other side of the membrane is kept sufficiently low. Oxygen permeable membrane technology eliminates the need for an oxygen plant and allows the integration of oxygen separation and reaction into a single process. Membranes can be shaped into hollow tube reactors, but other geometric shapes like honeycomb or corrugated forms are also possible.

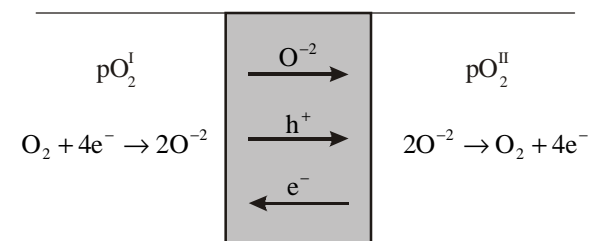


Fig. 1. Operating principle for an oxygen permeable membrane in a gradient of oxygen partial pressure ($pO_2^I > pO_2^{II}$)

2. Degradation of electrochemical ceramics. Recently, perovskite ceramics exhibiting both high ionic and electronic conductivity have been given much attention for applications in high-temperature electrochemical devices. For example, perovskites $(La, Sr)MnO_3$ and $La_{1-x}Sr_xFeO_3$ are candidate materials for cathode in solid oxide fuel cells [7], and $LaCrO_3$ has been intensively studied for the use as an interconnect material [4]. Perovskite ceramics have also a potential application as dense oxygen permeable membranes for partial oxidation of natural gas or for separation of oxygen from air [2, 6, 12].

The degradation of electrochemical ceramics with time is a major problem for its applications in high-temperature electrochemical devices. The degradation due to chemical expansion, creep deformation and formation of non-conductive secondary phases on interfaces between different materials or on the surface has a strong effect on the microstructure, mechanical and functional properties of electrochemical ceramics.

The degradation of electrochemical ceramics with time can be investigated experimentally. The chemical expansion observed in electrochemical ceramics at high temperature occurs in addition to the thermal expansion [13]. This chemically-induced swelling can be considered as a general phenomenon concerning all mixed-valence materials that compensate for the reduction of cations by creating anion vacancies.

The chemical expansion of perovskite $\text{La}_{0.6}\text{Sr}_{0.4}\text{Co}_{0.2}\text{Fe}_{0.8}\text{O}_{3-d}$ (d is oxygen non-stoichiometry) at the temperature of 800°C as a function of partial pressure of oxygen can be found in Fig. 2 [14]. The experimental data are shown by symbols while the assumed extrapolated behaviour is shown by dashed line. For example, the chemical expansion of perovskite $\text{La}_{0.6}\text{Sr}_{0.4}\text{Co}_{0.2}\text{Fe}_{0.8}\text{O}_{3-d}$ with oxygen pressure of 5 atm was measured to 0.3 %. Thus, it is necessary to take into account chemically- induced swelling considering the degradation of electrochemical ceramics with time.

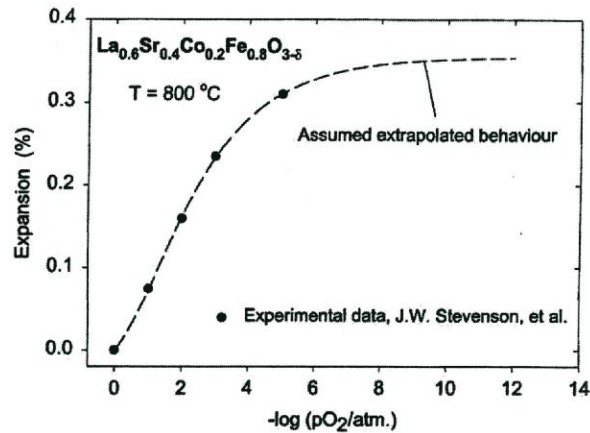


Fig. 2. Chemical expansion of perovskite $\text{La}_{0.6}\text{Sr}_{0.4}\text{Co}_{0.2}\text{Fe}_{0.8}\text{O}_{3-d}$ at 800°C

Another feature of electrochemical ceramics with applications in SOFCs and OPMs is their creep behaviour related to the diffusion of the various defects (cations and anions) in the crystal [15-19]. Anion diffusion could be by oxygen vacancies or oxygen interstitials depending on the composition of the material [20, 21]. Grain boundaries are particularly likely to be affected by the presence of defects [22]. The rates of mass transport processes such as creep, grain growth or densification can be controlled either by the effective diffusion coefficient of the slowest moving species [22, 23] or by the concentration of the slowest moving species [23, 24]. For example, the creep process in yttrium aluminium garnet polycrystals in the temperature range 1400°C - 1550°C is controlled by ytterbium cation diffusion [25]. Diffusion of cations controls also compressive creep performance of perovskite SrFeO_3 in the temperature range 800°C - 1000°C [26]. This is contrary to the creep behaviour of $\text{La}_{0.2}\text{Sr}_{0.8}\text{Fe}_{0.8}\text{Cr}_{0.2}\text{O}_{3-d}$ at low partial pressure of oxygen explained by the effect of the cluster concentration [27-30].

One of the creep features of a large class of structural ceramics is their differ-

ent behavior in tension and compression. This creep feature may be investigated experimentally by comparing creep curves obtained from uniaxial tests in tension and compression at the same temperature and taking specimens at the same orientation from the body under consideration. In this way it is established for polycrystalline ceramics that the absolute values of creep strain, chosen for one and the same absolute value of constant stress, and for one and the same value of time, are essentially different depending on the sign of the stress. Thus, one has two different creep curves (one in tension, and the other in compression). For example, the growth of the absolute value of the creep strain with time in an yttria-containing hot-isostatically- pressed silicon nitride in the temperature range 1316°C - 1399°C under uniaxial tension and uniaxial compression is reported in [31]. It is seen from Fig. 3 that the creep strain rate in the secondary stage of the creep curves for tension and compression at 1316°C and with the absolute value of the stress of 125 MPa is different by a factor of about six. Furthermore, the creep strain rate at the steady state under tension at 1371°C and with 200 MPa is approximately 20 times larger than that in compression while the corresponding creep rupture times are different by a factor of about three.

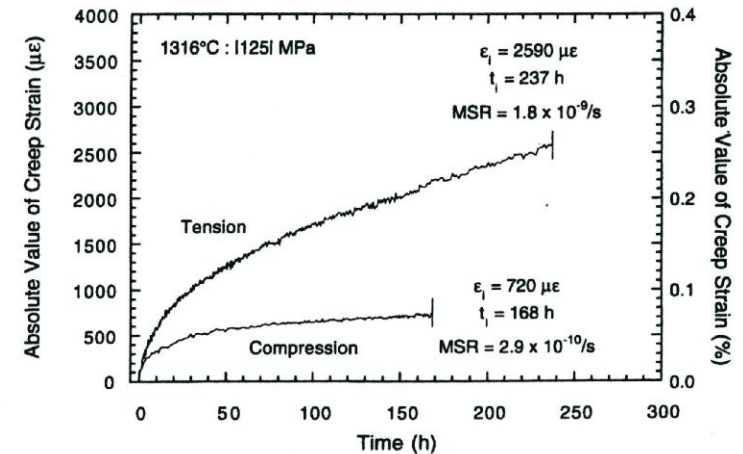


Fig. 3. Creep curves in an yttria-containing hot-isostatically- pressed silicon nitride under tension and compression at 1316°C and with the absolute value of the stress of 125 MPa

Alternatively, tension/compression creep asymmetry for electrochemical ceramics can be determined experimentally by measuring residual stresses in a specimen after bending with creep conditions and using laser technique.

Chemically- induced swelling without creep in ceramic oxygen ion- conducting membranes has been studied in [3, 32]. The thermal creep (without diffusion) in the structures of different shape and geometry has been considered in [33-58]. However, to the best authors' knowledge, up to now no investigations exist of

chemically- induced swelling with diffusional creep and creep damage development in SOFCs as well as in OPMs. In addition, substantially higher fracture toughness can be expected, due to diffusional crack blunting and possibly crack healing [30]. A general approach to the analysis of creep, chemical expansion, creep damage and lifetime reduction in SOFCs has been proposed earlier in [59]. The specific objectives of the present paper are:

- to develop a new approach in detail to a three- dimensional stress- strain state in SOFCs and OPMs based on simultaneous coupling of the diffusion theory with swelling, creep and creep damage analysis incorporating the diffusion coefficient of oxygen ions, the volume diffusion coefficient of the slowest moving species, grain- boundary diffusion coefficient and concentration of the various defects (cations and anions) in the crystal in order to control macroscopic properties of electrochemical ceramics at elevated temperatures by manipulations at the atomic and molecular levels,
- to develop an integrated micro-meso-macro constitutive framework for swelling and diffusional creep in electrochemical ceramics with multiaxial stress state using Fick's second law, and taking into account different creep behavior of materials in tension and compression,
- to do the identification of the material parameters in a nonlinear constitutive model,
- to formulate the initial/ variational problems for swelling, diffusional creep and damage development in SOFCs and OPMs that will be used to predict the time changing of the induced stresses and lifetime of plate, shell and three-dimensional structures of different shape and geometry operating under severe service load conditions as well as at elevated temperatures, and to quantify the functional properties and degradation of electrochemical ceramics.

3. Modeling of SOFCs and OPMs. In general, the problem under discussion for the three-dimensional body (volume V , bounded by surface $S = S_1 + S_2$) (Fig. 4) with reference to the Cartesian coordinates x_i ($i = \overline{1,3}$) for the case of the small strains and zero volume forces can be formulated as a variational problem of minimizing the following functional of Lagrange:

$$L(\dot{\mathbf{u}}, \dot{\mathbf{e}}, \dot{\mathbf{p}}) = 0.5 \iiint_V [C_{klmn} (\dot{\mathbf{e}}_{kl} - \dot{\mathbf{r}}_{kl} - \dot{\mathbf{p}}_{kl}) (\dot{\mathbf{e}}_{mn} - \dot{\mathbf{r}}_{mn} - \dot{\mathbf{p}}_{mn})] dV - \iint_{S_2} \dot{\mathbf{X}}_{nj} \dot{\mathbf{u}}_j dS \quad (1)$$

where the dot above the symbol denotes a derivative with respect to time. The body under consideration is under the action of the surface forces $\dot{\mathbf{X}}_{nj}$ applied to part of the surface S_2 . Displacements of the surface points

$$u_i = u_i^* \quad (2)$$

are given on the remainder of the surface S_1 . The components of the total inini-

tesimal strain tensor \mathbf{e}_{kl} are assumed to be the sum of the elastic components e_{kl} , chemically- induced components r_{kl} and the creep ones p_{kl} , i.e.

$$\mathbf{e}_{kl} = e_{kl} + r_{kl} + p_{kl} \quad (3)$$

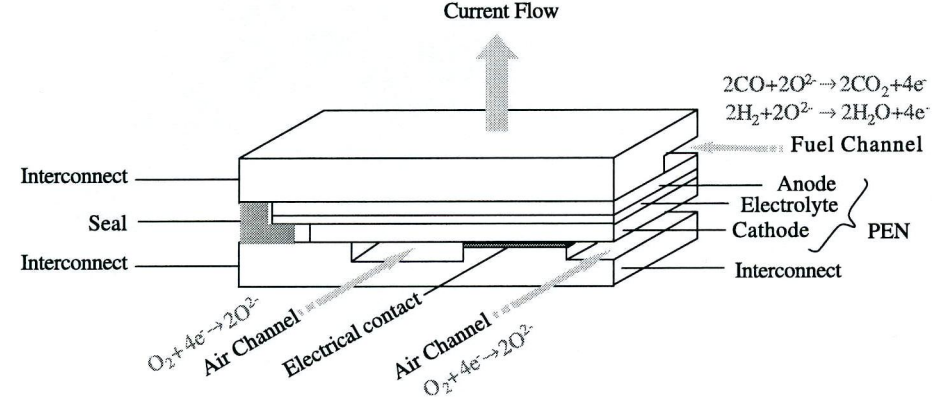


Fig. 4. Schematic of a repeat unit for a planar SOFC stack design [61]

The components of the stress tensor can be defined according to the generalized Hooke's law:

$$\mathbf{s}_{ij} = C_{ijkl} \mathbf{e}_{kl} \quad (4)$$

with the elastic material parameter tensor given for the isotropic material as follows

$$C_{ijkl} = \frac{E}{2(1-n^2)} [(d_{ik}d_{jl} + d_{il}d_{jk})(1-n) + 2nd_{ij}d_{kl}] \quad (5)$$

where \mathbf{s}_{kl} is the Cauchy stress tensor, \mathbf{d}_{kl} is the Kronecker delta, E is the Young's modulus and n is the Poisson's ratio. The components of the strain tensor and the components of the displacement vector are related to the kinematic equations

$$\mathbf{e}_{kl} = \frac{1}{2} (u_{k,l} + u_{l,k}). \quad (6)$$

The components of the chemically- induced strain tensor can be defined as

$$\mathbf{r}_{kl} = R C d_{kl} \quad (7)$$

where R is a material parameter. Concentration of oxygen ions C can be found by integration of the Fick's second law using some initial and boundary conditions. The components of the diffusional creep strain rate tensor can be described by the

following equation [60]

$$\dot{\mathbf{d}}_{kl} = f(s_e) C^* \left(\frac{3 P S_{kl}}{2 S_i} + M d_{kl} \right) \quad (8)$$

where S_i is the stress intensity, S_{kl} is the stress deviator, s_e is the equivalent stress, $s_e = P S_i + M S_{kl} d_{kl}$, $f(s_e)$ is some function of the equivalent stress that can be determined, for example, as $f(s_e) = 1 - \exp(-s_e^k / H)$, P , M , H and k are material parameters, C^* is cluster concentration [27-30] or the concentration of the slowest moving species [23, 24] that can be found incorporating the effective diffusion coefficient and integrating Fick's second law with some initial and boundary conditions. In order to describe the damage growth, it is possible to introduce the Kachanov-Rabotnov damage parameter [54] $j \in [0, 1]$. An initial value $j = 0$ corresponds to reference state while a critical value $j = 1$ corresponds to creep rupture time. Creep damage growth can be described by the following evolution equation [60]

$$\frac{dj}{dt} = [1 - \exp(-s_e^m / \bar{L})] \frac{j^{-b}}{(1-j)^q} \quad (9)$$

where \bar{L} , m , q and b are material parameters. Constitutive equation (8) and kinetic equation (9) describe different creep behaviour and different damage development under tensile and compressive loading types.

Material parameters of a constitutive model proposed can be found using the "parameter identification" by minimization of a least squares functional containing differences between measured and numerical calculated comparative quantities. The optimization of the objective function has been carried out using the Levenberg-Marquardt algorithm.

The problem under discussion is the physically nonlinear initial/variational problem. Minimizing the functional given by Eq. (1) must be considered simultaneously with the initial value problem (with respect to time) for the physical equations of swelling and creep as well as for diffusion. This leads to the problem to find such displacement rates that yield an extremal value of the functional in Eq. (1) assuming that components of the creep strain rate tensor $\dot{\mathbf{d}}_{ij}$ and components of

the chemically-induced strain rate tensor $\dot{\mathbf{d}}_{ij}$ are given as some known functions of the coordinates at each fixed instant of time. The diffusion equation can be discretized using a classical second-order centered scheme. The fourth-order Runge-Kutta-Merson's method with automatical selection of time step sizes [33, 45, 47, 59] has been used in order to solve the initial value problem for swelling and creep. The combination of the Finite Element Method and R-functions theory [62-64] has been used in order to obtain the numerical solution of linearized three-dimensional problems. Using the R-functions method the boundary conditions at the air channel

and fuel channel (Fig. 4) will be satisfied exactly.

Below is given a number of particular cases related to different designs of solid oxide fuel cells and oxygen permeable membranes.

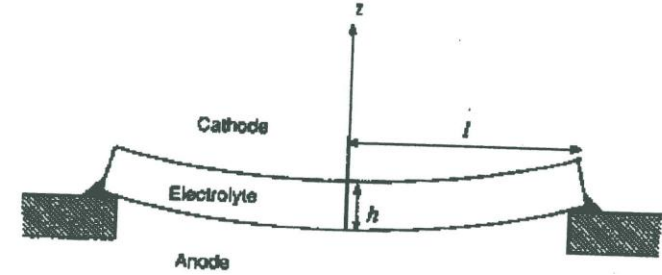


Fig. 5. Schematic diagram showing the electrolyte of solid oxide fuel cells in fully relaxed case [3]

1) The thin plate with reference to the Cartesian coordinates x_1, x_2 and z occupies the domain W on plane $x_1 O x_2$ with the boundary ∂W . The bending problem of the thin plate at large displacements (Fig. 5) is related to minimizing the following functional of Lagrange

$$\begin{aligned} I(\mathbf{u}_1, \mathbf{u}_2, w) = & 0.5 \iint_W \int_h [\mathbf{d}_{kl} (\mathbf{d}_{kl} - \dot{\mathbf{d}}_{kl} - \dot{\mathbf{d}}_{kl}) + s_{11} \mathbf{u}_1^2 + s_{22} \mathbf{u}_2^2 + \\ & + 2s_{12} \mathbf{u}_1 \mathbf{u}_2] dx_1 dx_2 dz - \iint_W \mathbf{q}_z w dx_1 dx_2 - \\ & - \int_{\partial W_2} [P_n^{(1)} (\mathbf{u}_1 n_1 + \mathbf{u}_2 n_2) + P_t^{(1)} (\mathbf{u}_2 n_1 - \mathbf{u}_1 n_2)] d\partial W \end{aligned} \quad (10)$$

where u_1 and u_2 are the components of the displacement of the coordinate plane, w is the normal displacement, $(\dots)_1 = \frac{\partial(\dots)}{\partial x_1}$, $(\dots)_2 = \frac{\partial(\dots)}{\partial x_2}$,

$n_1 = \cos(\mathbf{n}, x_1)$, $n_2 = \cos(\mathbf{n}, x_2)$, \mathbf{n} is the external normal to the boundary ∂W_2 at each its point, $P_n^{(1)}$ and $P_t^{(1)}$ are the normal and tangential components of the contour forces, h is the thickness of the plate, q_z is the surface load in the normal direction. There are different formulations of the multilayer plate theory [65]. In order to take into account the bending of the plate at large displacements and large rotations the functional of Lagrange proposed in [66] can be also considered.

2) The tubular symmetrical about the axis z ceramic membrane (Fig. 6) with

reference to the cylindrical coordinate system (r , q and z) occupies the domain W on plane rOz with the boundary ∂W . The functional of Lagrange can be formulated as follows

$$\begin{aligned}
 I(\mathfrak{u}_r, \mathfrak{u}_z) = & 0.5 \iint_W \left[I_1 \left(\mathfrak{u}_{r,r}^2 + \mathfrak{u}_{z,z}^2 + \frac{\mathfrak{u}_r^2}{r^2} \right) + G(\mathfrak{u}_{r,z} + \mathfrak{u}_{z,r})^2 \right. \\
 & \left. + 2I \left(\mathfrak{u}_{r,r} \mathfrak{u}_{z,z} + \frac{\mathfrak{u}_r(\mathfrak{u}_{r,r} + \mathfrak{u}_{z,z})}{r} \right) \right] r dr dz - \\
 & - \iint_W \left[\mathfrak{u}_{r,r} \mathfrak{N}_r^c + \mathfrak{u}_{z,z} \mathfrak{N}_z^c + \frac{\mathfrak{u}_r \mathfrak{N}_q^c}{r} + \mathfrak{N}_{rz}^c (\mathfrak{u}_{r,z} + \mathfrak{u}_{z,r}) \right] r dr dz - \\
 & - \int_{\partial W_2} (\mathfrak{N}_n^0 \mathfrak{u}_n + \mathfrak{N}_t^0 \mathfrak{u}_t) d\partial W
 \end{aligned} \tag{11}$$

where

$$\begin{aligned}
 \mathfrak{N}_r^c &= [I_1(\mathfrak{u}_r + \mathfrak{u}_{rr}) + I(\mathfrak{u}_{zz} + \mathfrak{u}_{qq} + \mathfrak{u}_{zz} + \mathfrak{u}_{qq})], \\
 \mathfrak{N}_z^c &= [I_1(\mathfrak{u}_z + \mathfrak{u}_{zz}) + I(\mathfrak{u}_{rr} + \mathfrak{u}_{qq} + \mathfrak{u}_{rr} + \mathfrak{u}_{qq})], \quad \mathfrak{N}_{rz}^c = 2G\mathfrak{u}_{rz}, \\
 \mathfrak{N}_q^c &= [I_1(\mathfrak{u}_q + \mathfrak{u}_{qq}) + I(\mathfrak{u}_{rr} + \mathfrak{u}_{zz} + \mathfrak{u}_{rr} + \mathfrak{u}_{zz})], \quad \mathfrak{u}_n = \mathfrak{u}_r n_1 + \mathfrak{u}_z n_2, \quad \mathfrak{u}_t = \mathfrak{u}_z n_1 - \mathfrak{u}_r n_2, \\
 I &= \frac{En}{(1-2n)(1+n)}, \quad I_1 = I + 2G,
 \end{aligned}$$

G is the modulus of elasticity in shear.

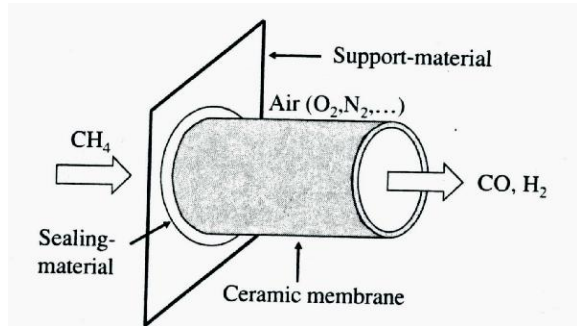


Fig. 6. Schematic of an oxygen permeable membrane system used for direct conversion of methane to syngas [12]

The numerical determination of solution in the particular cases based on Eqs. (10) and (11) is similar to that of Eq. (1).

The future research will be related to the incorporation of the constitutive and numerical framework developed in this paper into the ANSYS codes in a form of the computer-based structural modeling tool.

The research described in this paper was funded by the Alexander von Humboldt Foundation, Germany. The first author would like to thank Mrs. Isakova Tatyana Vladimirovna for help, useful advices and support.

References: 1. *Minh N.Q.* Ceramic fuel cells. J. Am. Ceram. Soc. -1993.- 76.- PP.563-588. 2. *Fossdal A.* Phase relations, thermal and mechanical properties of LaFeO₃-based ceramics. Ph.D Thesis, Norwegian University of Science and Technology, Trondheim. -2003. 3. *Atkinson A.* Chemically induced stresses in gadolinium-doped ceria solid oxide fuel cell electrolytes. Solid State Ionics. -1997.- 95.- PP.249-258. 4. *Simmer S.P., Shelton J.P., Anderson M.D., Stevenson J.W.* Interaction between La(Sr)FeO₃ SOFC cathode and YSZ electrolyte. Solid State Ionics. -2003.- 161.- PP.11-18. 5. *Wolfenstine J.* Creep resistance comparison of two solid oxygen fuel cell electrolytes with the fluorite structure: cubic zirconia and doped-ceria. Journal of Power Sources. -2002.- 111.- PP.173-175. 6. *Petric A., Huang P., Tietz F.* Evaluation of La- Sr- Co- Fe- O perovskites for solid oxide fuel cells and gas separation membranes. Solis State Ionics. -2000.- 135.- PP.719-725. 7. *Simmer S.P., Bonnett J.F., Canfield N.L., Meinhardt K.D., Shelton J.P., Sprengle V.L., Stevenson J.W.* Development of lanthanum ferrite SOFC cathodes. Journal of Power Sources. -2003.- 113.- PP.1-10. 8. *Gutierrez-Mora F., Ralph J.M., Roubort J.L.* High-temperature mechanical properties of anode-supported bilayers. Solid State Ionics. -2002.- 149.- PP.177-184. 9. *Atkinson A., Selcuk A.* Mechanical behaviour of ceramic oxygen ion-conducting membranes. Solid State Ionics. -2000.- 134.- PP.59-66. 10. *Hendriksen P.V., Larsen P.H., Mogensen M., Poulsen F.W., Wik K.* Prospects and problems of dense oxygen permeable membranes. Catalysis Today. -2000.- 56.- PP.283-295. 11. *Kharton V.V., Naumovich E.N., Nikolaev A.V.* Materials of high-temperature electrochemical oxygen membranes. Journal of Membrane Science. - 1996.- 111.- PP.149-157. 12. *Faaland S.* Heterogeneous ceramic interfaces in solid oxide fuel cells and dense oxygen permeable membranes. Ph.D Thesis, Norwegian University of Science and Technology, Trondheim. -2000. 13. *Adler S.B.* Chemical expansivity of electrochemical ceramics. J. Am. Ceram. Soc. -2001.- 84.- PP.2117-2119. 14. *Stevenson J.W., Armstrong T.R., Pedersen L.R., Weber W.J.* //Anderson H.U., Khandkar A.C., Liu M. (Eds.), Proceedings of the First International Symposium on Ceramic Membranes. -The Electrochemical Society, 1995. 15. *Akashi T., Nanko M., Maruyama T., Shiraishi Y., Tanabe J.* Solid- state reaction kinetics of LaCrO₃ from the oxides and determination of La³⁺ diffusion coefficient. J. Electrochem. Soc. -1998.- 145.- PP.2090-2094. 16. *Crouch A.G., Robertson J.* Creep and oxygen diffusion in magnetite. Acta Metall. Mater. -1990.- 38.- PP.2567-2572. 17. *Haneda H.* A study of defect structures in oxide materials by secondary ion mass spectrometry. Applied Surface Science. -2003.- 203-204.- PP.625-629. 18. *Yasuda I., Hishinuma M.* Chemical diffusion in polycrystalline calcium-doped lanthanum chromites. Journal of Solid State Chemistry. -1995.- 115.- PP.152-157. 19. *Yasuda I., Hishinuma M.* Electrical conductivity and chemical diffusion coefficient of strontium-doped lanthanum manganites. Journal of Solid State Chemistry. -1996.- 123.- PP.382-390. 20. *Atkinson A., Chater R.J., Rudkin R.* Oxygen diffusion and surface exchange in La_{0.8}Sr_{0.2}Fe_{0.8}Cr_{0.2}O_{3-d} under reducing conditions. Solid State Ionics. -2000.- 139.- PP.233-240. 21. *Yasuda I., Ogasawara K., Hishinuma M., Kawada T., Dokiya M.* Oxygen tracer diffusion coefficient of (La- Sr)MnO_{3-d}. Solid State Ionics. -1996.- 86-88.-PP. 1197-1201. 22. *Harding J.H., Atkinson K.J.W., Grimes R.W.* Experiment and theory of diffusion in alumina. J. Am. Ceram. Soc. -2003.- 86.-PP.554-559. 23. *Roubort J.L., Goretta K.C., Cook R.E., Wolfenstine J.* Deformation of perovskite electronic ceramics- a review. Solid State Ionics. -2000.- 129.- PP.53-62. 24. *Sagdahl L.T., Einarsrud M.-A., Grande T.* Sintering of LaFeO₃ Ceramics. J. Am. Ceram. Soc. - 2000.- 83.-PP. 2318-2320. 25. *Jimenez-Melendo M., Haneda H.* Ytterbium cation diffusion in yttrium aluminium garnet (YAG)- implications for creep mechanisms. J. Am. Ceram. Soc. -2001.- 84.- PP.2356-2360. 26. *Kleveland K., Wereszczak A., Kirkland T.P.* Compressive creep performance of SrFeO₃. J. Am.Ceram. Soc. -2001.- 84.- PP.1822-1826. 27. *Majkic G., Jacobson*

A.J., Salama K. Stress-induced diffusion and defect chemistry of $\text{La}_{0.2}\text{Sr}_{0.8}\text{Fe}_{0.8}\text{Cr}_{0.2}\text{O}_{3-d}$. Part 3. Defect-chemistry based modelling. *Solid State Ionics*.-2004.- 167.- PP.255-262. **28.** *Majkic G., Mironova M., Wheeler L.T., Salama K.* Stress-induced diffusion and defect chemistry of $\text{La}_{0.2}\text{Sr}_{0.8}\text{Fe}_{0.8}\text{Cr}_{0.2}\text{O}_{3-d}$ Part 2. Structural, elemental and chemical analysis. *Solid State Ionics*.- 2004.- 167.- PP.243-254. **29.** *Majkic G., Wheeler L.T., Salama K.* High-temperature deformation of $\text{La}_{0.2}\text{Sr}_{0.8}\text{Fe}_{0.8}\text{Cr}_{0.2}\text{O}_{3-d}$ mixed ionic-electronic conductor. *Solid State Ionics*.- 2002.- 146.- PP.393-404. **30.** *Majkic G., Wheeler L.T., Salama K.* Stress-induced diffusion and defect chemistry of $\text{La}_{0.2}\text{Sr}_{0.8}\text{Fe}_{0.8}\text{Cr}_{0.2}\text{O}_{3-d}$ Part 1. Creep in controlled-oxygen atmosphere. *Solid State Ionics*.-2003.- 164.- PP.137-148. **31.** *Wereszczak A.A., Ferber M.K., Kirkland T.P., Barnes A.S., Frome E. L., Menon M.N.* Asymmetric tensile and compressive creep deformation of hot-isostatically-pressed Y_2O_3 -Doped- Si_3N_4 . *J. Eur. Ceramic Soc.*- 1999.- 19.- PP.227-237. **32.** *Atkinson A., Ramos T.M.G.M.* Chemically induced stresses in ceramic oxygen ion-conducting membranes. *Solid State Ionics*.- 2000.- 129.-PP. 259-269. **33.** *Altenbach H., Zolochovsky A.* Creep of thin shells by consideration of the anisotropic materials and the different behavior in tension and compression. *Forsch. Ingenieurwesen*.-1991.- 57.- PP.172-179. **34.** *Axenenko O., Tsvelikh A.* A hybrid finite element approach to the solution of creep problems. *Comp. Materials Sci.*-1996.- 6.- PP.268-280. **35.** *Bathe K.J.* Finite Elements Procedures.- New York: Prentice Hall, Englewood Cliffs, 1996. **36.** *Becker A.A., Hyde T.H., Xia L.* Numerical analysis of creep in components. *J. Strain Anal.*-1994.-29.- PP.27-34. **37.** *Bellenger E., Bussy P.* Phenomenological modeling and numerical simulation of different modes of creep damage evolution. *Int. J. Solids Structures*.- 2001.- 38.- PP.577-604. **38.** *Betten J.* Creep Mechanics.- Berlin: Springer-Verlag, 2002. **39.** *Bodnar A., Chrzanowski M.* A non-unilateral damage in creeping plates //Zyczowski, M. (Ed.), *Creep in Structures*.-Berlin: Springer-Verlag, 1991.- PP.287-293. **40.** *Boyle J.T., Spence J.* Stress Analysis for Creep.-London: Butterworths, 1983. **41.** *Chen G.G., Hsu T.R.* A mixed explicit-implicit (El) algorithm for creep stress analysis. *Int. J. Num. Meth. Engng.*-1988.- 26.- PP.511-524. **42.** *Hayhurst D.R.* Stress redistribution and rupture due to creep in a uniformly stretched thin plate containing a circular hole. *Trans. ASME. J. Appl. Mech.*-1973.- 40.- PP.253-260. **43.** *Hayhurst D.R.* The prediction of creep-rupture times of rotating discs using biaxial damage relationships. *Trans. ASME. J. Appl. Mech.*-1973.- 40.- PP.88-95. **44.** *Hayhurst D.R., Dimmer P.R., Chernuka M.W.* Estimates of the creep rupture lifetime of structures using the finite element method. *J. Mech. Phys. Solids*.- 1975.- 23.- PP.335-355. **45.** *Hayhurst D.R., Dimmer P.R., Morrison G.J.* Development of continuum damage in the creep rupture of notched bars. *Trans. R. Soc. London*.-1984.- A 311.- PP.103-129. **46.** *Hyde T.H., Xia L., Becker A.A.* Prediction of creep failure in aeroengine materials under multiaxial stress states. *Int. J. Mech. Sci.*-1996.- 38.- PP.385-403. **47.** *Ling L., Tu S.-T., Gong J.-M.* Application of Runge-Kutta-Merson algorithm for creep damage analysis. *Int. J. Press. Vessel Piping*. 2000.- 77.- PP.243-248. **48.** *Mahnken R.* Creep simulation of asymmetric effects by use of stress mode dependent weighting functions. *Int. J. Solids Structures*.- 2003.- 40.- PP.6189-6209. **49.** *Murakami S., Liu Y.* Mesh-dependence in local approach to creep fracture. *Int. J. Damage Mech.*-1995.- 4.- PP.230-250. **50.** *Murakami S., Liu Y., Mizuno M.* Computational methods for creep fracture analysis by damage mechanics. *Comput. Methods Appl. Mech.Engng.*-2000.- 183.- PP.15-33. **51.** *Othman A.M., Dyson B.F., Hayhurst D.R., Lin J.* Continuum damage mechanics modelling of circumferentially notched tension bars undergoing tertiary creep with physically-based constitutive equations. *Acta. Metall. Mater.*-1994.- 42.- PP.597-611. **52.** *Penny R.K., Marriott D.L.* Design for Creep.- London: Chapman and Hall, 1995. **53.** *Qi W., Brocks W., Bertram A.* An FE-analysis of anisotropic creep damage and deformation in the single crystal SRR99 under multiaxial loads. *Comp. Materials Sci.*-2000.- 19.- PP.292-297. **54.** *Rabotnov Yu.N.* Creep Problems in Structural Members. -Amsterdam: North-Holland, 1969. **55.** *Saanouni K., Chaboche J.L., Bathias C.* On the creep –crack growth predictions by a local approach. *Engg. Fract. Mech.*-1986.- 25.- PP.677-691. **56.** *Simo J.C., Hughes T.J.R.* Computational Inelasticity.- New York: Springer-Verlag, 1998. **57.** *Smith S.D., Webster J.J., Hyde T.H.* Three-dimensional damage calculations for creep crack growth in 316 stainless steel //Allison I.M., Ruiz C. (Eds.), *Applied Solid Mechanics*. – Amsterdam: Elsevier, 1989. **58.** *Zolochovsky A. A.* Allowance for differences in tension and compression for materials in the creep problems of shells. *Dynamics and Strength of Machines*.-Kharkov, 1980. –№ 32. – PP. 8-13. **59.** *Zolochovsky A. A., Hyde T.H., Hu Zhaoji.* An integrated approach to the analysis of creep, chemical expansion, creep damage and lifetime reduction for solid oxide fuel cells // Вісник НТУ «ХПІ». Тем. вип.: Машиноведение и САПР. – 2007. – № 3. – С. 151-159. **60.** *Betten J., Sklepus A., Zolochovsky A.* A constitutive theory for creep behavior of initially isotropic materials

sustaining unilateral damage. *Mechanics Research Communications*. – 2003. – 30. – PP.251-256. **61.** *Yang Z., Stevenson J.W., Meinhardt K.D.* Chemical interactions of barium-calcium-aluminosilicate-based sealing glasses with oxidation resistant alloys. *Solid State Ionics*. – 2003. – 160. – PP.213-225. **62.** *Rvachev V.L.* Analytical description of some geometric objects. *Dokl. AN USSR*. – 1963. – 153. – PP.765-768. **63.** *Rvachev V.L., Sheiko T.I.* R-functions in boundary value problems in mechanics. *Appl. Mech. Rev.* - 1995. – 48. – PP.151-188. **64.** *Zolochovsky A.A., Rvachev V.L. and Sklepus S.N.* Variational-structural method in creep problems. *Mathematical Methods and Physical-Mechanical Fields*. – 2001. – 44. – №.1. – PP.80-85. **65.** *Kühhorn A., Golze M.* Thickness flexible theory with generalized core warping for plane sandwich structures //Kienzler R., Altenbach H., Ott I. (Eds.), *Theories of Plates and Shells, EUROMECH Colloquium 444, Lecture Notes in Applied and Computational Mechanics*. – Berlin: Springer-Verlag, 2004, V.16. – PP.100-108. **66.** *Stoffel M., Schmidt R., Weichert D.* Simulation and experimental validation of the dynamic response of viscoplastic plates //Villacampa Esteve Y., Carlomagno G.M., Brebbia C.A. (Eds.), *Computational Methods and Experimental Measurements*. Southampton: WIT Press, 2001. – PP.206-210.

Поступила в редколлегию 12.07.07

УДК 539.3

A. ZOLOCHEVSKY, Dr. Sc., NTU “KPI”, **G. THIAGARAJAN**, Dr.,
University of Missouri-Kansas City, USA

AN INTEGRATED APPROACH TO ASSESSING SEISMIC SIMULATION BASED ON ANALYSIS OF PRESEISMIC, COSEISMIC, POSTSEISMIC AND INTERSEISMIC CREEP, AND CREEP DAMAGE EVOLUTION

Теоретичні та чисельні дослідження даної роботи направлено на дослідження Parkfield землетрусів. Головні дослідження направлено на пояснення впливу фізичної та хімічної дифузії, деформації повзучості в досейсмічному, сейсмічному, післясейсмічному та міжсейсмічному періодах, включаючи сталу стадію повзучості, дифузійної повзучості, циклічної та динамічної повзучості, великих деформацій, асиметрії повзучості при розтягу та стисканні, явища ділатансії, активного та пасивного розвитку пошкоджуваності, циклічних варіацій крайових умов, історії тектонічних навантажень, сейсмічної активності земної кори на формування розломів та розривів кори та відповідно на виникнення катастрофічних випадків. Основні дослідження сфокусовано на дослідженні того, як дифузія, досейсмічна, сейсмічна, післясейсмічна та міжсейсмічна повзучість, великі деформації, розвиток процесів пошкоджуваності та заліковування, рух фронту руйнування, крайові умови можуть бути змодельовані для розуміння Parkfield землетрусів та прогнозування нових руйнівних землетрусів.

In this paper, a comprehensive theoretical, numerical and computational investigation based on the analysis of the Parkfield earthquakes will be carried out with the main focus directed at the understanding on how physical and chemical transport phenomena, creep deformation with preseismic, coseismic, postseismic and interseismic periods including steady-state static creep, diffusional creep, cyclic creep and dynamic creep, large strains, tension/compression creep asymmetry, creep dilatancy, active creep damage state (degradation) and passive creep damage state (healing), cyclic variations of velocities in boundary conditions, and tectonic loading history affect fault sliding, seismic activity in the crust surrounding a fault including accelerated seismic release characterized by cumulative Benioff strain, spatio-